Extended self-similarity and dissipation range dynamics of three-dimensional turbulence

Anirban Sain[1] and J. K. Bhattacharjee[2]
[1]*Department of Physics, Simon Fraser University, Burnaby, British Columbia, Canada V5A 1S6*
[2]*Department of Theoretical Physics, Indian Association for Cultivation of Science, Jadavpur, Calcutta 700 032, India*
(Received 22 January 1999)

We carry out a self-consistent calculation of the structure functions in the dissipation range using the Navier-Stokes equation. Combining these results with the known structures in the inertial range, we actually propose crossover functions for the structure functions that take one smoothly from the inertial to the dissipation regime. These crossover functions are shown to exhibit extended self-similarity properties consistent with experimental findings. [S1063-651X(99)12207-4]

PACS number(s): 47.27.Gs, 05.45.−a, 05.70.Jk, 47.27.Eq

I. INTRODUCTION

The inertial-range multiscaling of the velocity structure functions in fully developed homogeneous, isotropic turbulence has been investigated extensively [1–8]. By comparison the asymptotic behaviors of the structure functions in the far dissipation range have been less well studied. In this paper we report a self-consistent, approximate, analytical calculation of the behaviors of structure functions in the dissipation range. By using accepted scaling forms for the structure functions in the inertial range, we propose asymptotic forms for them in the dissipation range. We also propose forms for the crossover from the inertial- to dissipation-range asymptotic behaviors and demonstrate how extended self-similarity (ESS) can be understood.

II. CALCULATION AND RESULTS

We work with the forced three-dimensional Navier-Stokes (NS) equation (3DNSE)

$$\dot{v}_i(\mathbf{k})+\nu k^2 v_i(\mathbf{k})=-iM_{ijl}(\mathbf{k})\sum_{\mathbf{p}} v_j(\mathbf{p})v_l(\mathbf{k}-\mathbf{p})+f_i(\mathbf{k},t), \tag{1}$$

where $M_{ijl}=[k_jP_{il}(\mathbf{k})+k_lP_{ij}(\mathbf{k})]/2$, the transverse projector $P_{ij}=\delta_{ij}-k_ik_j/k^2$, and the external force f_i is stochastic, has zero mean, and $\langle \mathbf{f}_i(\mathbf{k},t)\mathbf{f}_j(\mathbf{k}',t')\rangle = D(k)P_{ij}(\mathbf{k})\delta(\mathbf{k}+\mathbf{k}')\delta(t-t')$. $D(k)$ sharply decays to zero beyond the integral scale (L^{-1}). [For what follows we do not need the specific functional form of $D(k)$]. This stochastic force maintains the energy balance in the inertial range. The energy input per unit time ($\overline{\epsilon}$) at long wavelengths cascades through different length scales because of the nonlinear term, and for $k>k_d$, is dissipated by molecular viscosity (ν), where $k_d=(\overline{\epsilon}/\nu^3)^{1/4}$. In the inertial range $L^{-1}\ll k\ll k_d$

$$S_{2n}\sim k^{-(\zeta_{2n}+3n)}, \tag{2}$$

where the structure functions $S_{2n}(k)$=connected part of $\langle |v(k)|^{2n}\rangle$. We can define $\langle |v(k)|^{2n}\rangle$ as the Fourier transform of a real-space correlation function in the following way:

$$\langle |v(k)|^{2n}\rangle = \int \langle \mathbf{v}(\mathbf{x_1})\cdot\mathbf{v}(\mathbf{x_1}+\mathbf{r_1})\mathbf{v}(\mathbf{x_2})\cdot\mathbf{v}(\mathbf{x_2}+\mathbf{r_2}) \cdots \mathbf{v}(\mathbf{x_n})\cdot\mathbf{v}(\mathbf{x_n}+\mathbf{r_n})\rangle \prod_{j=1}^{n}\left(\frac{d\mathbf{x}_j}{L^3}d\mathbf{r}_j e^{i\mathbf{k}\cdot\mathbf{r}_j}\right).$$

The exponent ζ_n is $n/3$ in the Kolmogorov, 1941 (K41) [1] theory. In general ζ_n differs from $n/3$ and one of the best estimates of the deviation $\delta\zeta_n$, due to She and Leveque (SL) [10], is

$$\delta\zeta_n=\zeta_n-n/3=-\frac{2n}{9}+2\left[1-\left(\frac{2}{3}\right)^{n/3}\right]. \tag{3}$$

Here we investigate the behavior of S_{2n} in the dissipation range. Our principal results are summarized below, for $D=3$ and for $k\gg K$:

$$S_2(k)\sim k^{-1}e^{-k/K},$$
$$S_4(k)\sim k^{-5}e^{-2k/K}, \tag{4}$$
$$S_{2n}(k)\sim k^{-3n}e^{-nk/K},\quad n\geqslant 3$$

where $\delta_2=2-D$ (in this section we use D for dimension of space) and $K=O(k_d)$. By studying the correction to the above result in powers of K/k, we propose (in $D=3$) the following crossover function (that crosses over from the dissipation- to the inertial-range form):

$$S_2(k)\sim\frac{1}{k}\left(1+\alpha_1\left[\frac{K}{k}\right]^m\right)^{(2+\zeta_2)/m}e^{-k/K}, \tag{5}$$

where α_1 is a number of $O(1)$, and

$$S_4(k)\sim\frac{1}{k^5}\left(1+\alpha_2\left[\frac{K}{k}\right]^m\right)^{(1+\zeta_4)/m}e^{-2k/K},$$
$$S_{2n}(k)\sim k^{-3n}\left(1+\alpha_n\left[\frac{K}{k}\right]^m\right)^{\zeta_{2n}/m}e^{-nk/K},\quad n\geqslant 3. \tag{6}$$

Note that, in the region $K/k\gg 1$ (i.e., the inertial range), this form reduces to Eq. (2) and, in the region $K/k\ll 1$ (i.e., the dissipation range), this reduces to Eq. (4). The constants α_n are nonuniversal and will be shown to be almost indepen-

dent of n. An approximate analytic evaluation of m gives $m=1$. A more accurate numerical evaluation of m yields $m<1$. The explicit crossover forms that we have written down help us understand the idea of extended self-similarity introduced by Benzi *et al.* [11]. Our approach is an alternative to that of Segel *et al.* [12]. If we expand Eq. (6), for $m=1$, about the inertial-range form Eq. (2), we note that

$$S_{2n}(k)\sim k^{-(\zeta_{2n}+3n)}\left(1-\left[n-\frac{\zeta_{2n}}{\alpha_n}\right]\frac{k}{K}\right), \tag{7}$$

so the simple power-law form will break down when

$$k\sim\frac{\alpha_n}{n\alpha_n-\zeta_{2n}}K. \tag{8}$$

Various studies [13,14,16] suggest that, when S_{2n} deviates from its inertial-range behavior, it first increases beyond the $k^{-(\zeta_{2n}+3n)}$ line and then, at even larger values of k [$\sim O(k_d)$], it falls off sharply when k is in the dissipation range. This initial flattening of the energy spectrum is known as the ''bottleneck effect'' in the literature [13,14,16]. We incorporate this effect in our expression for S_{2n} by demanding that the coefficient of the term k/K in Eq. (7) be positive. This leads to a constraint on α_n, namely,

$$\zeta_{2n}>n\alpha_n. \tag{9}$$

Note that, as we go further away from the inertial range ($K/k\lesssim 1$), the exponential factor dominates and causes the rapid fall of the structure function S_{2n}. For the structure function S_2, this condition becomes

$$\alpha_1<2+\zeta_2. \tag{10}$$

(Note, however, that if $\alpha_n<0$, the bottleneck hump goes away. Our choice $\alpha_n>0$ is purely phenomenological in nature.) We notice that $\zeta_{2n}-n\alpha_n$ increases with n if we constrain $\alpha_n<2/9$. This follows from the fact that ζ_{2n} is a monotonically increasing, convex function of n and $\zeta_{2n}\to 2n/9$ as $n\to\infty$. With these bounds on α_n, a few phenomenological results follow, which can be checked analytically also.

(1) As n increases, the structure functions $S_{2n}(k)$ deviate from the inertial-range power-law behavior at smaller and smaller values of k/K [17].

(2) The position of the ''bottleneck'' hump shifts towards smaller values of k/K as n increases. Consequently the ultimate exponential falloff occurs at lower and lower values of k/K for higher and higher n. These two effects are clearly demonstrated in Fig. 1.

We now turn to ESS. From Eq. (6) it is clear that

$$\begin{aligned}S_{2n}(k)&\sim\{S_{2m}(k)\}^{(\zeta_{2n}+3n)/(\zeta_{2m}+3m)}\\&\times\left[e^{-nk/K}e^{m[(\zeta_{2n}+3n)/(\zeta_{2m}+3m)]k/K}\right.\\&\left.\times\frac{[1+\alpha_n^{-1}k/K]^{\zeta_{2n}}}{[1+\alpha_m^{-1}k/K]^{\zeta_{2m}[(\zeta_{2n}+3n)/(\zeta_{2m}+3m)]}}\right]\\&\sim\{S_{2m}(k)\}^{(\zeta_{2n}+3n)/(\zeta_{2m}+3m)}[d(k)].\end{aligned} \tag{11}$$

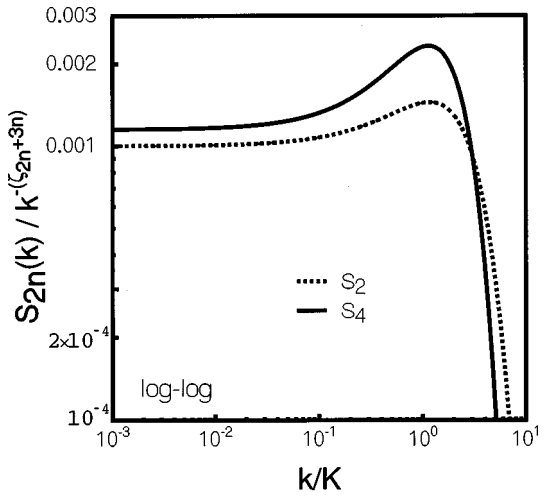

FIG. 1. Log_{10}-log_{10} plot of $S_{2n}/k^{-(\zeta_{2n}+3n)}$ versus k/K. To obtain this plot we have used Eq. (6) and the SL formula for ζ_{2n}. We have chosen $\alpha_n=\alpha_1=1/9$, which is consistent with the constraint on α_n. The curves for $n=2$ and $n=4$ have been shifted along the vertical axis by arbitrary scale factors to compare them clearly. The humps are a clear manifestation of the bottleneck effect.

The first term in the braces in Eq. (11) leads to a straight line in the log-log ESS plots and its slope is related to the inertial-range multiscaling exponents. The second term in the large square brackets in Eq. (11) causes deviation from this straight line. Note first that the two exponential factors combine to yield a term $\exp(-\mu_{n,m}k/K)$ that decays much more weakly than $\exp(-nk/K)$ (if we use the K41 value $\zeta_{2n}=2n/3$, the two exponential factors cancel exactly to yield 1). From Eq. (11) we see that $\mu_{n,m}=n-m(\zeta_{2n}+3n)/(\zeta_{2m}+3m)$ and, if we use the SL formula, we can easily verify that for $n>m$, $n-m\geqslant\mu_{n,m}\geqslant 0$, whence $\exp(-nk/K)\ll\exp(-\mu_{n,m}k/K)$, for $k/K\gg 1$. (This follows from the property that ζ_n increases monotonically with n, but with a slope that decreases as n increases and hence $\delta\zeta_n/\delta\zeta_m>n/m$.) [Clearly $\mu_{n,n}=0$ and, as $(n-m)$ increases with m fixed (as in typical ESS plots), $\mu_{n,m}$ increases, leading to increasingly strong deviations from the inertial-range line.] In a conventional log-log plot of $S_{2n}(k)$ versus k, the exponential factor that modifies the power-law dependence in the inertial range behaves as $\exp(-nk/K)$ for $k/K\gg 1$. Hence the apparent inertial range is extended in ESS plots. Also the variation of $[1+\alpha_n^{-1}k/K]^{n(3+\delta_2)+\zeta_{2n}}$ which causes weak deviation from power-law behavior is muted by the denominator (as α_n's have been assumed to have the same sign and shown to be almost independent of n later). These points are shown clearly in Fig. 2, which shows the following.

(1) In ESS plots the effect of the exponential damping factor sets in at higher value of k/K than in log-log plots of S_{2n} versus k plots. This can be seen by a comparison of Fig. 1 and Fig. 2. Figure 1 shows that the inertial-range region in a log-log plot of S_{2n} versus k/K extends to $k/K\simeq 10^{-1}$. Figure 2 shows that the damping factor $d(k)$ in the ESS form [Eq. (11)] is significant for $k/K>1$; thus an ESS plot should yield an extension of the apparent inertial range by nearly one order of magnitude.

(2) Note also that the log-log ESS plot of S_6 versus S_2 deviates from inertial-range behavior at a lower value of k/K

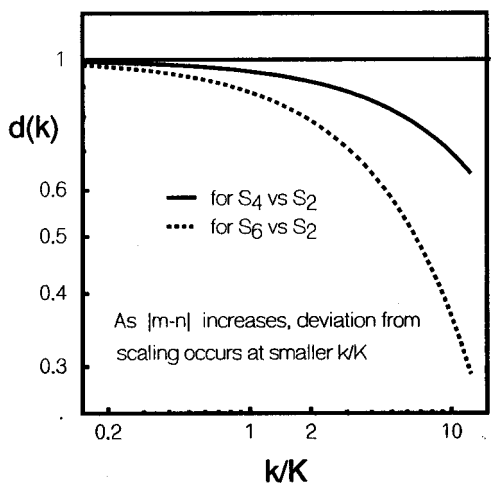

FIG. 2. Log_{10}-$\log_{10}$ plot of the damping factor $d(k)$ versus k/K, when the damping factor is the explicit k-dependent coefficient of $S_2 m(k)^{(\zeta_{2n}+3n)/(\zeta_{2m}+3m)}$ in our Eq. (11). We have chosen $\alpha_n=\alpha_1=1/9$, consistent with the constraint on α_n.

than its S_4 versus S_2 analogue.

We first note that the correlation functions in the dissipation range fall off extremely fast [18] beyond the characteristic scale k_d; consequently there is no divergence in the self-energies and correlation functions for $k>k_d$. Thus the viscosity coefficient ν does not acquire any scale-dependent renormalization. One-loop self-consistent perturbation theory yields [5,6]

$$S_2(k,\omega)=|G(k,\omega)|^2k^2\int_{p,|\mathbf{k}-\mathbf{p}|\geqslant k_d}\frac{d^Dp}{(2\pi)^D}\frac{d\omega'}{2\pi}\times a(\mathbf{k},\mathbf{p},\mathbf{k}-\mathbf{p})S_2(|\mathbf{k}-\mathbf{p}|,\omega-\omega')S_2(p,\omega'). \tag{12}$$

(See Fig. 3.)

On the right-hand side the tree-level term $D(k)|G|^2$ has been dropped because the forcing amplitude $D(k)\to 0$ for $k>L^{-1}$. The angular factor $a(\mathbf{k},\mathbf{p},\mathbf{k}-\mathbf{p})=\frac{1}{2}(1-xyz-2y^2z^2)$; when the trio $(\mathbf{k},\mathbf{p},\mathbf{k}-\mathbf{p})$ forms a triangle and x,y,z are the direction cosines of the angles opposite to $\mathbf{k},\mathbf{p}$, and $\mathbf{k}-\mathbf{p}$, respectively. The inverse of the response function $G^{-1}=-i\omega+\nu k^2$ and the correlation function $S_2(k,\omega)=k^{\delta_2}f(k/k_d)\nu k^2/(\omega^2+\nu^2k^4)$, such that

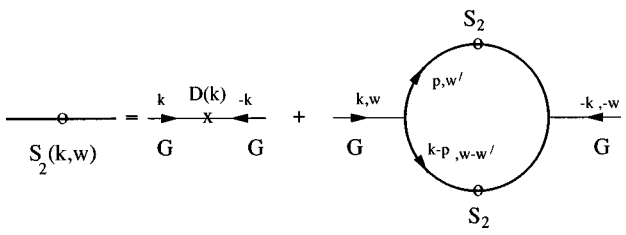

FIG. 3. A graphical representation of our one-loop, self-consistent approximation Eq. (12). $D(k)$ is the amplitude of the noise variance, G denotes the renormalized response function, and S_2 the renormalized correlation function.

$$\int\frac{dw}{2\pi}S_2(k,\omega)=S_2(k,t=0)=k^{\delta_2}f(k/k_d). \tag{13}$$

The form $S_2(k,\omega)=k^{\delta_2}\nu k^2f(k/k_d)/(\omega^2+\nu^2k^4)$ that we have used here, is tantamount to considering the linearized effective equation (for the dissipation range)

$$\dot{v}_i(\mathbf{k})+\nu k^2v_i(\mathbf{k})=f_i(\mathbf{k},t)$$

when the external noise has a variance

$$\langle\mathbf{f}_i(\mathbf{k},t)\mathbf{f}_j(\mathbf{k}',t')\rangle=Ak^{\delta_2}\nu k^2f(k/k_d)\times P_{ij}(\mathbf{k})\,\delta(\mathbf{k}+\mathbf{k}')\,\delta(t-t').$$

Though there is no external forcing in the dissipation range, the indirect forcing through the nonlinear term has been replaced by the noise term.

Note that in Eq. (12) we have used k_d as the lower cutoff of the integral. Strictly speaking, given the form of the nonlinear term in the 3DNSE, all modes $v_i(\mathbf{k})$ interact with each other. However, since (a) we are interested in the regime $k/K\gg 1$, the far dissipation range here and (b) the cascade picture suggests locality of interactions in k space, we ignore the interactions of the far dissipation range modes with those below k_d. (Compare, e.g., interactions only between nearest-neighbor and next-nearest-neighbor shells in the Gledzer-Okhitani-Yamada GOY shell model [17].)

To compare the two sides of Eq. (12), we make use of a saddle-point approximation in evaluating the integral on the right-hand side of Eq. (12). In this approximation it turns out that $f(k/k_d)=e^{-\beta k/k_d}$, where $K=k_d/\beta$. That this is a self-consistent solution can be checked by working with the exponential factors on the right-hand side of Eq. (12) in terms of a shifted wave number $\mathbf{q}\equiv(\mathbf{k}/2-\mathbf{p})$ as follows:

$$\begin{aligned}e^{-\beta p/k_d}e^{-\beta|\mathbf{k}-\mathbf{p}|/k_d}&=e^{-\beta(|\mathbf{k}/2-\mathbf{q}|+|\mathbf{k}/2+\mathbf{q}|)/k_d}\\&=e^{-\beta([k^2/4+q^2-\mathbf{k}\cdot\mathbf{q}]^{1/2}+[k^2/4+q^2+\mathbf{k}\cdot\mathbf{q}]^{1/2})/k_d}\\&=e^{-\beta k/k_d}e^{-\beta k/k_d[q^2\sin^2\theta/k^2+O(q^4/k^4)+\cdots]},\end{aligned} \tag{14}$$

where q and θ are the integration variables. Now the saddle-point approximation amounts to setting the factor multiplying $e^{-\beta k/k_d}$ equal to unity, the maximum value of the factor. The exponential factor on the left-hand side of Eq. (9) is thus reproduced and power counting of the rest yields

$$\delta_2=-(D-2). \tag{15}$$

To check the correctness of this self-consistent solution we numerically integrated (over $\mathbf{p}$) the right-hand side of Eq. (12) for $D=3$, with lower cutoff k_d, and using the form $S_2(k,\omega)=b_0[\nu k^2/(\omega^2+\nu^2k^4)]e^{-k/k_d}/k$. At zero external frequency ($\omega=0$), we have called the resulting integral $I_d(k)$ (see below). The comparison of $I_d(k)$ with $b_0(1/k)e^{-k/k_d}$ is shown in Fig. 4(a) (we chose $K=k_d$ in our numerical work). The agreement is good for $k/k_d\geqslant 20$ (i.e., $k\gg k_d$). Note that, for a given value of k_d, self-consistency fixes the value of b_0.

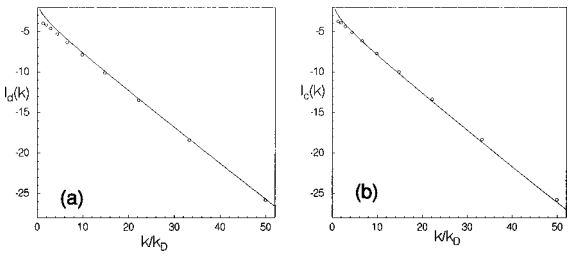

FIG. 4. Plots of (a) $\log_{10}[I_d(k)]$ and (b) $\log_{10}[I_c(k)]$ versus k/k_d. Circles show data from our numerical evaluation of these integrals $I_d(k)$ and $I_c(k)$. Solid lines denote (a) $(b_0/k)e^{-k/k_d}$ and (b) $(b_0/k)(k_d/k)^{1/4}e^{-k/k_d}$, respectively.

To study the crossover behavior from the dissipation range to the inertial range, we need to include the first correction to the large k/K behavior described above. We do this by assuming that the correction to $S_2(k)$ can be expanded in powers of $(K/k)^m$ and thus, in $D=3$,

$$S_2(k)=\frac{b_0}{k}[1+b_1(K/k)^m]e^{-k/K}, \tag{16}$$

where m is an unknown power to be determined later. We substitute this form of $S_2(k)$ into the right-hand side of Eq. (12) (here $S_2(k,\omega)\sim[\nu k^2/(\omega^2+\nu^2k^4)]S_2(k)$) and retain terms up to linear order in b_1. After integrating over ω', the right-hand side of Eq. (12), considered at zero external frequency ($w=0$), turns out to be proportional to (see Appendix A)

$$\int_{p,|\mathbf{k}-\mathbf{p}|\geqslant k_d}\frac{d^3p}{(2\pi)^3}a(\mathbf{k},\mathbf{p},\mathbf{k}-\mathbf{p})\frac{e^{-(p+|\mathbf{k}-\mathbf{p}|)/K}}{(p^2+|\mathbf{k}-\mathbf{p}|^2)p|\mathbf{k}-\mathbf{p}|}$$
$$\times[1+b_1(K/p)^m+b_1(K/|\mathbf{k}-\mathbf{p}|)^m]$$
$$\equiv I_d(k)+b_1I_c(k), \tag{17}$$

where $I_d(k)$, defined earlier, does not depend on b_1, the b_1-dependent part is denoted by $b_1I_c(k)$, and subscripts d and c stand for dominant and correction, respectively. The self-consistency [of Eqs. (16) and (17)] requires that $I_d=b_0(1/k)e^{-k/K}$ and $I_c=b_0(1/k)(K/k)^me^{-k/K}$, for any value of b_1. So far the value of m has not been determined.

We first estimate m in an approximate way. The requirement that $I_c(k)$ be finite leads to $m<2$. If we write $m=2-\epsilon$, we can evaluate the integral I_c to the leading pole [19] in ϵ. I_c can be evaluated by using a saddle-point technique; the dominant contribution comes from $p\simeq k$. The final result must be of the form $[1+b_1(K/p)^m]$ for self-consistency; so, at the level of approximation just described, we find $m=1$. Thus, for $k\gg k_d$, $S_2\propto(1/k)(1+b_1K/k)e^{-k/K}$ and, for $k\ll k_d$ (the inertial range), $S_2\propto k^{-(3+\zeta_2)}$. The simplest interpolating form between the two behaviors is Eq. (5).

Our value for m above is approximate, because the integral in Eq. (17) involves a lower cut-off k_d, which we did not consider in our analysis. So when k/k_d is not very large, we expect deviation from the value $m=1$. This led us to determine m numerically by evaluating the correction integral $I_c(k)$ and demanding that it be consistent with $b_0(1/k)(k_d/k)^me^{-k/K}$. Figure 4(b) shows a comparison between the numerically evaluated $I_c(k)$ (circles) and our analytic approximation for it with $m=1/4$. So our earlier approximation overestimates m. For this value of m the match is the closest. Note that the agreement is good for $k/k_d\geqslant 7$. All our earlier arguments demonstrating the ESS properties of S_n hold good as long as $m>0$. Note that the fact that I_c fits better than I_d up to relatively small k/k_d does not mean that the correction term improves the fit. In Fig. 4, I_d and I_c are separately compared to the respective terms in Eq. (16) because, as mentioned earlier, b_1 cannot be determined from our formalism. In the numerical integration of $I_c(k)$, we have used the same values for the parameters k_d and b_0 which we obtained from the self-consistency requirement of $I_d(k)$.

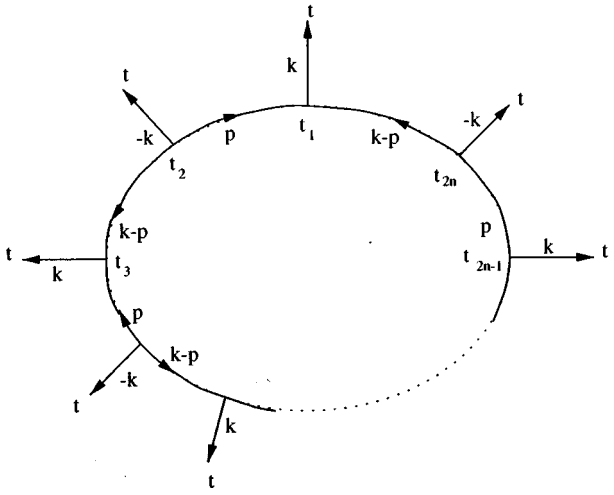

FIG. 5. The diagram contributing to $S_{2n}(k)$ in the dissipation regime. All the internal lines in the diagram represent correlation functions $S_2(p;t_j,t_{j+1})$ and all external lines represent propagators $G(k;t,t_j)$, etc. The respective momentum arguments of the G and S_2's are indicated on the diagram.

It should be noted that, in the far dissipation range that we are considering here, the single-loop–self-consistency approximation is sufficient. We have checked that the contributions from two-loop diagrams are at most of the same order as the single-loop diagram. So their inclusion just changes the amplitude of $S_2(k)$. This statement is true for the evaluation of S_{2n} $(n>1)$ also, which we carry out below. Out of the various possible arrangements of the $\mathbf{k}$ and $-\mathbf{k}$ external legs on a one-loop diagram, we evaluate the most relevant one (shown in Fig. 5). Contributions from other possible one-loop diagrams are exponentially smaller and hence their contributions are negligible. The contribution from Fig. 5 is

$$S_{2n}(k,t)=\langle[v(\mathbf{k},t)v(-\mathbf{k},t)]^n\rangle$$
$$\sim k^{2n}\int_{-\infty}^{t}dt_1\cdots\int_{-\infty}^{t}dt_{2n}\int\frac{d^Dp}{(2\pi)^D}G(k;t,t_1)$$
$$\times G(-k;t,t_2)G(k;t,t_3)\cdots G(-k;t,t_{2n})$$
$$\times S_2(p,|t_1-t_2|)S_2(|\mathbf{k}-\mathbf{p}|,|t_2-t_3|)$$
$$\times S_2(p,|t_3-t_4|)\cdots S_2(|\mathbf{k}-\mathbf{p}|,|t_{2n}-t_1|). \tag{18}$$

As $S_2(k,t)\sim k^{-(D-2)}e^{-k/K}e^{-|t|\nu k^2}$, we note that the inte-

gral of Eq. (18) will be dominated by the low momentum pole at $p=k$. Using a pole approximation for evaluating the integral, a momentum count produces the result that $S_{2n}(k,t)\propto k^{-3n}e^{-nk/K}$ (see Appendix B). This establishes Eq. (4). Within our formalism we cannot show that Eq. (4) holds for odd moments also, but we assume it does for the sake of monotonicity. Now we note that Eq. (4) implies $S_n \sim k^{-2n}S_2^n$, i.e., a deviation from simple scaling in the far dissipation range. But this is not of the kind ($S_n \sim S_3^{\alpha_n}$) which has been reported in direct numerical simulation (DNS) studies [9]. This disparity indicates that higher-order corrections to our approximation might be important.

We now study the first deviation of S_{2n} from its form in Eq. (4). To do so, we introduce the first deviation of $S_{2n}(k,t)$ in Eq. (18). The integral in Eq. (18) is already dominated by the low momentum pole; hence the additional correction part is also dominated by this pole. There are n contributions of equal strength from each of the $S_2(p)$ and $S_2(|\mathbf{k}-\mathbf{p}|)$ and consequently for $k\gg K$,

$$S_{2n}\propto k^{-3n}[1+b_n(K/k)^m]e^{-nk/K}, \tag{19}$$

where $b_n\propto nb_1$. Since the quantity ζ_{2n} in Eq. (6) is roughly proprtional to n (neglecting weak deviations from $2n/3$), we consequently infer that in the interpolation formula of Eq. (6), the constant α_n is independent of n, to a leading approximation of the present analysis. Thus the main results, Eqs. (4)–(6), are obtained.

Now we look at the real-space structure function $S_2(r)=\langle[\mathbf{v}(\mathbf{x}+\mathbf{r})-\mathbf{v}(\mathbf{x})]^2\rangle$; this is the inverse Fourier transform of $2[u_0^2\delta(k)-S_2(k)]$ (where $u_0^2/2$ is the mean energy). For r in the far dissipation range, $S_2(r)$ will be determined principally by our $k\gg k_d$ form of $S_2(k)$ [i.e., $\sim(1/k)e^{-k/K}$]. This yields $S_2(r)\approx c_1 r^2+O(r^4)$. Here c_1 is a function of ν and $\overline{\epsilon}$. This form of $S_2(r)$ is consistent with the result of Sirovich *et al.* [20]. The added advantage of our k-space calculation is its ability to predict the asymptotic forms of higher-order structure functions [$S_{2n}(k),\ n>1$].

III. DISCUSSION AND CONCLUSIONS

In summary, we have shown that by considering the Navier-Stokes equation and carrying out a self-consistent treatment of the k-space structure functions we can establish their asymptotic forms in the dissipation range. By computing the first correction to these asymptotic forms and in addition using well-known results about the inertial range, we can construct explicit crossover functions for the structure functions (crossover from $k\gg k_d$ to $k\ll k_d$). Also the present theory gives a description of the crossover behavior that is consistent with ESS.

As far as the bottleneck effect is concerned we should point out that the effect is built by hand into our interpolation forms Eqs. (5) and (6) by imposing constraints on α_n; it is not a consequence of our theory. We refer the reader to Refs. [13,14,16] for other work on the bottleneck effect. She and Jackson [16] have suggested an empirical curve-fitting formula [Eq. (4) in their paper]. For the far dissipation range $k\gg k_d$ it reads

$$E(k)=E(k_p)\alpha\left(\frac{k}{k_p}\right)^{-\beta}e^{-\mu k/k_p}.$$

This is similar to our Eq. (5) but the exponent β in their Eq. (4) differs from ours; but our exponent follows from a self-consistent treatment. As far as the value of this exponent β is concerned the issue is far from settled because three studies [15,16,20] quote three differenet values, namely, -3.3, 1, and $-5/3$, respectively. Our value for this exponent is -1, which is closest to that of Sirovich *et al.* Interestingly their analysis starts in r space and gets, for small r, $S_2(r)\sim r^2$, which is the same as ours. We believe β cannot be determined unambiguously by only data fitting, because, in the far dissipation range, the exponential factor dominates strongly.

ACKNOWLEDGMENTS

We would like to thank R. Pandit (of IISc Bangalore, India) for discussions and useful comments, P. Pradhan for help in drawing the Feynman diagrams, and CSIR (India) for support. A.S. would like to thank NSERC (Canada) for support.

APPENDIX A: DERIVATION OF EQ. (17) FROM EQ. (12)

Below we show the detailed derivation of Eq. (14). We determined the unknown exponent m of the leading correction to the $k\gg K$ form of $S_2(k)$ numerically by demanding self-consistency of the following equation [our Eq. (12)]:

$$S_2(k,\omega)=|G|^2k^2\int\frac{d^Dp}{(2\pi)^D}\frac{d\omega'}{2\pi}a(\mathbf{k},\mathbf{p},\mathbf{k}-\mathbf{p})\times S_2(|\mathbf{k}-\mathbf{p}|,\omega-\omega')S_2(p,\omega').$$

More explicitly the right-hand side

$$=|G|^2k^2\int\frac{d^Dp}{(2\pi)^D}\frac{d\omega'}{2\pi}\times\frac{a\nu^2p^2|\mathbf{k}-\mathbf{p}|^2e^{-(p+|\mathbf{k}-\mathbf{p}|)/k}}{(\omega'^2+\nu^2p^4)([\omega-\omega']^2+\nu^2|\mathbf{k}-\mathbf{p}|^4)}\frac{1}{p|\mathbf{k}-\mathbf{p}|}.$$

Now we integrate over ω' and set $\omega=0$. Below we suppress the ω'-independent part of the integral and show the result of ω' integration on the explicitly ω'-dependent part. The poles lie at $\omega'=\pm i\nu p^2$ and $\omega'=\omega\pm i\nu p^2$. Integrating over the upper half plane we get

$$\frac{2\pi i}{2i\nu(2\pi)}\left(\frac{1}{p^2([\omega-i\nu p^2]^2+\nu^2|\mathbf{k}-\mathbf{p}|^4)}+\frac{1}{|\mathbf{k}-\mathbf{p}|^2([\omega+i\nu|\mathbf{k}-\mathbf{p}|^2]^2+\nu^2p^4)}\right)$$

$$=\frac{1}{2\nu^3(|\mathbf{k}-\mathbf{p}|^4-p^4)}\left(\frac{1}{p^2}-\frac{1}{|\mathbf{k}-\mathbf{p}|^2}\right)\quad\text{for}\ \ \omega=0.$$

After simplifying the above expression, inserting $|G(k,\omega=0)|^2=1/\nu^2k^4$, and then putting together all the factors, the integral reduces to

$$\int \frac{d^Dp}{(2\pi)^D}a(\mathbf{k},\mathbf{p},\mathbf{k}-\mathbf{p})\frac{b_0^2}{2\nu^3k^2}\frac{e^{-(p+|\mathbf{k}-\mathbf{p}|)/K}}{(p^2+|\mathbf{k}-\mathbf{p}|^2)p|\mathbf{k}-\mathbf{p}|}, \tag{A1}$$

which is precisely the $O(b_1^0)$ term in Eq. (17), barring a factor of $1/k^2$. This factor gets cancelled with the left-hand side, hence

$$S_2(k,\omega=0)=\frac{b_0}{\nu k^2}\left(\frac{e^{-k/K}}{k}\right)=\frac{1}{\nu k^2}[S_2(k)]. \tag{A2}$$

In our numerics we have used $\nu=1$.

APPENDIX B: CALCULATION OF S_{2n}

We start from Eq. (18) here (also see Fig. 5).

$$\begin{aligned}S_{2n}(k,t)&=\langle[v(\mathbf{k},t)v(-\mathbf{k},t)]^n\rangle\\&\sim k^{2n}\int_{-\infty}^{t}dt_1\cdots\int_{-\infty}^{t}dt_{2n}\int\frac{d^Dp}{(2\pi)^D}G(k;t,t_1)\\&\times G(-k;t,t_2)G(k;t,t_3)\cdots G(-k;t,t_{2n})\\&\times S_2(p,|t_1-t_2|)S_2(|\mathbf{k}-\mathbf{p}|,|t_2-t_3|)\\&\times S_2(p,|t_3-t_4|)\cdots S_2(|\mathbf{k}-\mathbf{p}|,|t_{2n}-t_1|).\end{aligned}$$

Given the causal nature of $G(k;t,t_j)$, we have $t>t_j$ (the internal dummy indices) in the above expression. We substitute $S_2(k,t)\sim k^{\delta_2}e^{-k/K}e^{-|t|k^2}$ and $G(k;t,t')\sim e^{-k/K}e^{-(t-t')k^2}$ in the above expression. Here we have taken $\nu=1$. We carry out the momentum integral

$$\int d^3p\frac{1}{(|\mathbf{k}-\mathbf{p}|p)^n}e^{-n(p+|\mathbf{k}-\mathbf{p}|)/K}. \tag{B1}$$

For $n\geqslant 3$ this integral has equally strong divergences at $p=0$ and $\mathbf{p}=\mathbf{k}$. We avoid the divergences by assuming a lower cutoff $(=K)$ for the integral. So the dominant contribution for $k\gg K$ is

$$\sim e^{-nk/K}\frac{1}{k^n}. \tag{B2}$$

The following multiple time integral results from Eq. (18):

$$\begin{aligned}&\int_{-\infty}^{t}dt_1\cdots\int_{-\infty}^{t}dt_{2n}e^{-(t-t_1)k^2}\\&\times e^{-(t-t_2)k^2}e^{-(t-t_3)k^2}\cdots e^{-(t-t_{2n})k^2}e^{-p^2|t_1-t_2|}\\&\times e^{-|\mathbf{k}-\mathbf{p}|^2|t_2-t_3|}e^{-p^2|t_3-t_4|}\cdots e^{-|\mathbf{k}-\mathbf{p}|^2|t_{2n}-t_1|}.\end{aligned}$$

Because of the divergences mentioned above we evaluate this time integral at $\mathbf{p}=\mathbf{k}$. This approximation breaks up the time convolutions (which come from the correlation functions S_2) appearing in the integral and we get

$$\begin{aligned}&\sim\int_{-\infty}^{t}dt_1\cdots\int_{-\infty}^{t}dt_{2n}e^{-(t-t_1)k^2}e^{-(t-t_2)k^2}\\&\times e^{-(t-t_3)k^2}\cdots e^{-(t-t_{2n})k^2}e^{-(t-t_1)k^2}\\&\times e^{-(t-t_2)k^2}e^{-|t_1-t_2|k^2}e^{-|t_3-t_4|k^2}\cdots.\end{aligned} \tag{B3}$$

This is a product of n double integrals

$$\sim\left(\int_{-\infty}^{t}dt_1\int_{-\infty}^{t}dt_2e^{-(t-t_1)k^2}e^{-(t-t_2)k^2}e^{-|t_1-t_2|k^2}\right)^n. \tag{B4}$$

In the $t_1>t_2$ sector the integral reduces to

$$\begin{aligned}\left(\int_{-\infty}^{t}dt_1\int_{-\infty}^{t_1}dt_2e^{-2tk^2}e^{2t_2k^2}\right)^n&=\left(\frac{e^{-2tk^2}}{2k^2}\int_{-\infty}^{t}dt_1e^{2t_1k^2}\right)^n\\&=\left(\frac{1}{4k^4}\right)^n.\end{aligned}$$

Collecting all the k-dependent factors together, this leads to

$$S_{2n}(k,t)\sim\frac{k^{2n}k^{-n}}{k^{4n}}e^{-nk/K}\sim\frac{e^{-nk/K}}{k^{3n}}. \tag{B5}$$

APPENDIX C: CONTRIBUTION FROM THE ONE-LOOP DIAGRAM FOR $S_4(k)$

The momentum integral that results from the one-loop diagram for $S_4(k)$ is

$$k^4\int\frac{d^3p}{p^2|\mathbf{k}-\mathbf{p}|^2}e^{-(2p+2|\mathbf{k}-\mathbf{p}|)/K}. \tag{C1}$$

This integral does not have any infrared divergence. That becomes clear after performing the angular integral over θ. So we do not require a lower cutoff for this integral and hence allow interaction among all $p,|\mathbf{k}-\mathbf{p}|$ modes. (This statement is true for one-loop integrals for S_{2n}, for $n<3$.) In the above integral, we pull out the exponential factor using a saddle-point approximation, then scale out k from the integral and the rest of the integral in scaled variable p/k is a finite number. The dominant contribution of the above integral is

$$\simeq k^4\frac{1}{k}e^{-2k/K}. \tag{C2}$$

The time integral over internal time variables $t_1,t_2,\ldots,t_4$ produces $(1/k^2)^4$. So the net contribution of the one-loop diagram is

$$S_4(k)\sim\frac{e^{-2k/K}}{k^5}. \tag{C3}$$

[1] U. Frisch, *Turbulence: The Legacy of A.N. Kolmogorov* (Cambridge University Press, Cambridge, England, 1995).
[2] W. D. McComb, *The Physics of Fluid Turbulence* (Oxford University Press, Oxford, 1991).
[3] C. Meneveau and K. R. Sreenivasan, J. Fluid Mech. **224**, 429 (1991).
[4] V. S. L'vov and I. Procaccia, Phys. Rev. E **49**, 4044 (1994).
[5] C. Y. Mon and P. B. Weichman, Phys. Rev. Lett. **70**, 1101 (1993).
[6] J. K. Bhattacharjee, Phys. Fluids A **3**, 879 (1991).
[7] V. Yakhot and S. A. Orszag, J. Sci. Comput. **1**, 3 (1986).
[8] Sujan K. Dhar, Anirban Sain, Ashwin Pande, and Rahul Pandit, Pramana, J. Phys. **48**, 325 (1997), special issue on Nonlinearity and Chaos in Physical Sciences, edited by Ramakvishna Ramaswamy and K. R. Sreenivasan.
[9] Sujan K. Dhar, Anirban Sain, and Rahul Pandit, Phys. Rev. Lett. **78**, 2964 (1997).
[10] Z. S. She and E. Leveque, Phys. Rev. Lett. **72**, 336 (1994).
[11] R. Benzi, S. Ciliberto, R. Tripiccione, C. Baudet, F. Massaioli, and S. Succi, Phys. Rev. E **48**, R29 (1993).
[12] D. Segel, V. L'vov, and I. Procaccia, Phys. Rev. Lett. **76**, 1828 (1996).
[13] G. Falkovich, Phys. Fluids **6**, 1411 (1994). This theory is applicable only for $k<k_d$, whereas our analysis is valid only for $k>k_d$, i.e., for the dissipation range. Also this analysis is based on the energy flow equation, whereas our field theory method uses the one-loop self-consistent equation for S_{2n}.
[14] D. Lohse and A. Muller-Groeling, Phys. Rev. Lett. **74**, 1747 (1995).
[15] S. Chen *et al.*, Phys. Rev. Lett. **70**, 3051 (1993).
[16] Z. S. She and E. Jackson, Phys. Fluids A **5**, 1526 (1993).
[17] D. Pisarenko, L. Bieferale, D. Courvoisier, U. Frisch, and M. Vergassola, Phys. Fluids A **5**, 2533 (1993).
[18] R. H. Kraichnan, J. Fluid Mech. **5**, 497 (1959).
[19] J. K. Bhattacharjee and R. A. Ferrel, J. Math. Phys. **21**, 534 (1980).
[20] L. Sirovich, L. Smith, and V. Yakhot, Phys. Rev. Lett. **72**, 344 (1994).